Enhanced Optical Performance of $BaMgAl_{10}O_{17}$ Eu^{2+} Phosphor by a Novel Method of Carbon Coating

Yin, Liang Jun; Dong, Juntao; Wang, Yinping; Zhang, Bi; Zhou, Zheng Yang; Jian, Xian; Wu, Mengqiang; Xu, Xin; Van Ommen, J. Ruud; Hintzen, Hubertus T.

DOI
10.1021/acs.jpcc.5b10215

Publication date
2016

Document Version
Accepted author manuscript

Published in
The Journal of Physical Chemistry C

Accepted Author Manuscript. Link to published article: http://dx.doi.org/10.1021/acs.jpcc.5b10215 (ACS)

Enhanced Optical Performance of $BaMgAl_{10}O_{17}:Eu^{2+}$ Phosphor by a Novel Method of Carbon Coating

Liang-Jun Yin,[†] Juntao Dong,[†] Yinping Wang,[†] Bi Zhang,[‡] Zheng-Yang Zhou,[§] Xian Jian,**

[†] Mengqiang Wu,[†] Xin Xu,[‡] J. Ruud van Ommen,[#] and Hubertus T. (Bert) Hintzen[※]

[†]School of Energy Science and Engineering, University of Electronic Science and Technology of China, 2006 Xiyuan Road, Chengdu, 611731, P.R. China.
[‡]Laboratory of materials for energy conversion, Department of Materials Science and Engineering, University of Science and Technology of China, Hefei, 230026, P.R. China
[§]College of Chemistry and Molecular Engineering, Peking University, No.5 Yiheyuan Road, Beijing, 100871, P.R. China
[#]Department of Chemical Engineering, Faculty of Applied Sciences, Delft University of Technology, Julianalaan 136, 262 Delft, The Netherlands
[※]Luminescent Materials Research Group, Faculty of Applied Sciences, Delft University of Technology, Mekelweg 15, 2629 JB Delft, The Netherlands.

ABSTRACT: Many strategies have been adopted to improve thermal degradation of phosphors. Because of the stability and high transmittance of graphene, here we report a novel method of carbon coating on $BaMgAl_{10}O_{17}:Eu^{2+}$ (BAM) phosphor particles through Chemical Vapor Deposition (CVD). The chemical composition, microstructure, and luminescence performance of carbon-coated BAM were characterized carefully. This coating can be controlled within 3-10 atomic layers, depending on the reaction time. Due to the decrease of surface defects and the effective weakening effect of oxidizing Eu^{2+} to Eu^{3+} after

Liang-Jun Yin [†, ※]:
[†]School of Energy Science and Engineering, University of Electronic Science and Technology of China, 2006 Xiyuan Road, Chengdu, 611731, P.R. China.
[※]Luminescent Materials Research Group, Faculty of Applied Sciences, Delft University of Technology, Mekelweg 15, 2629 JB Delft, The Netherlands.

carbon coating, different layer numbers showed an obvious effect on the optical properties of carbon-coated BAM. Carbon-coated BAM phosphors had higher emission intensity and better oxidation resistance at high temperature than uncoated BAM phosphors. These results indicate that the method of carbon coating on phosphor particles is a promising way to improve the luminescence properties of other phosphors used in lighting and display devices.

INTRODUCTION

Barium magnesium aluminate $BaMgAl_{10}O_{17}$ activated by divalent europium ions Eu^{2+} (BAM) is one of excellent blue-emitting phosphors. It possesses high quantum efficiency (around 80%), good chromaticity, and strong absorption in the vacuum ultraviolet excitation band, making it widely used in three-band fluorescence lamps, plasma display panels (PDPs), and white light-emitting diode (LED).[1-4]

However, the oxidation resistance of BAM is rather poor. The BAM phosphor will undergo a decrease of luminescence intensity during post-treatment processes, for example, irradiation by ultraviolet photons, ion sputtering, and baking process in air during PDP manufacture. Especially, BAM phosphor will suffer from serious luminescence degradation due to the oxidation of luminescence centers Eu^{2+} when the heating temperature of BAM is raised to 500 – 700 °C.[4-7]

So far, many researchers have tried to enhance the oxidation resistance at high temperature of BAM phosphor, and many methods, such as coating, co-doping, compositional variation, and annealing in a non-oxidizing atmosphere, have been proposed.[5, 8-14] Among these methods, covering the phosphor particle surface with a coating is an effectively applied technique to enhance the chemical stability of BAM phosphor. Up to now, several inorganic materials have been reported as the coating materials such as SiO_2, MgO, Al_2O_3, $AlPO_4$, and $LaPO_4$ and so forth.[14-17] It is well known that Eu^{2+} is easily oxidized to Eu^{3+}, and all the materials mentioned above are oxides. Compared with carbon, these materials are more likely

to support an oxygen transportation channel and oxidize the luminescence centers Eu^{2+}, which contributes to luminescence degradation at higher treatment temperature. In addition, almost all the materials selected as the coating materials are coated by an emulsion method. The solution, which typically contains several additives, is mixed with BAM powders and stirred, centrifuged, filtered, washed with deionized water, and finally dried in an infrared-ray drying oven. It is difficult to precisely control the thickness of the coating by this method. In order to solve this problem, we use a CVD method to obtain carbon-coated BAM. By changing the gas flow rate and growth time, it is easy to get a series of thicknesses of the carbon coating. This work demonstrates for the first time the preparation of BAM phosphor powders with a thin carbon film. Besides, the microstructure of the phosphors and their luminescence properties are investigated.

EXPERIMENTAL SECTION

BAM powders were prepared by solid-state reaction from starting mixtures of $BaCO_3$, MgO, Al_2O_3 and Eu_2O_3 (99.99 wt%, Sinopharm Chemical Reagent Co. Ltd) in N_2 atmosphere at 1500 °C for 3 h. The average diameter of the prepared BAM particles is about 2.0 μm. Carbon coated BAM was prepared at 700 °C under gas mixtures of N_2 (gas flow rate: 100 ml/min) and C_2H_2 (gas flow rate: 30 ml/min). The process consists of the following four steps: (i) BAM was put in the quartz boat with a surface density of about 8.5 mg/cm^2; (ii) The quartz boat was put inside a conventional horizontal tube furnace. The temperature of the furnace was controlled at 700 °C for 30 min under N_2 atmosphere (gas flow rate: 100 ml/min); (iii) C_2H_2 gas (gas flow rate: 30 ml/min) was introduced into the tube for 1-5 min and (iv) Carbon-coated BAM was obtained after natural cooling of the sample in the furnace under N_2 atmosphere.

The phase formation was analyzed by an X-ray diffractometer (Model PW 1700, Philips, Eindhoven, The Netherlands) using Cu Kα radiation at a scanning rate of 2 °/min. The inner

structure was observed by Transmission Electron Microscopy (TEM) equipped with Energy Dispersion X-ray (EDX) spectrometer (Model 2100F, JEOL, Tokyo, Japan). Photoluminescence spectra were measured by a fluorescence spectrophotometer (Model F-4600, Hitachi, Tokyo, Japan) with a 200 W Xe lamp as an excitation source. The emission spectrum was corrected for the spectral response of the monochromator and Hamamatsu R928P photomultiplier tube (Hamamatsu Photonics K.K., Hamamatsu, Japan) by a light diffuser and tungsten lamp (Noma Electric Corp., NY; 10V, 4A). The excitation spectrum was also corrected for the spectral distribution of the Xe lamp intensity by measuring Rhodamine-B as a reference. Diffuse-reflectance spectra were measured at room temperature by a UV-Vis-NIR spectrophotometer (Model CARY 5000, Agilent Technologies, USA) equipped with an integrating sphere (Model Internal DRA-2500, Agilent Technologies, USA). The decay curves were measured at the room temperature by a combined steady-state lifetime fluorescence spectrophotometer (Model FLS920, Edinburgh Instruments, Edinburgh, U.K.). The internal and external quantum efficiency was measured using a QE-2100 spectrophotometer from Otsuka Photal Electronics.

RESULTS AND DISCUSSION

In order to study the chemical composition of the coating layer, EDS mapping analysis is shown in Figure 1. The Al, Mg, Ba atoms signals observed in the same concentrated area obviously represent the BAM host lattice. These elements are all even distributed in the BAM host lattice while the distribution of carbon shapes a thin layer around the BAM particle. This result clearly suggests that carbon has been successfully coated on the surface of BAM phosphor particles.

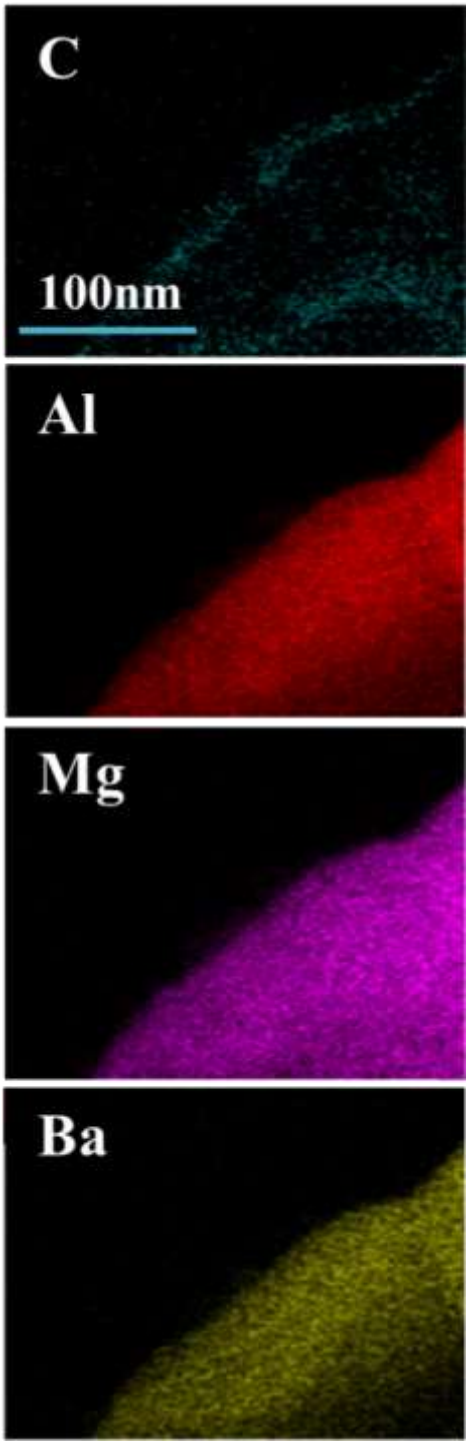

Figure 1. EDS mappings of C, Al, Mg, and Ba for a part of a carbon coated BAM particle with the reaction time 5 min.

Although it is convincingly shown that the coating layer is associated with carbon composition, the resolution of EDS mapping is still poor for determination of accurate structural characteristics. In the DF-STEM image, the contrast image reflects the difference of

atomic number and it is easy to distinguish the thin coating layer and BAM host. Figure 2 shows DF-STEM and HRTEM images of carbon coated BAM particle which exhibit the structure. On the basis of phase contrast, the DF-STEM image clearly indicates that the carbon compounds are densely coated on BAM phosphor powders. The coating layer of the products is estimated to have a thickness of 1.0-3.8 nm, which is dependent on the reaction time. With the increase of reaction time from 1 min to 5 min, the layer grows thicker and the number of defects decreases. Careful analysis of the HRTEM images indicates that there are three different thicknesses of the carbon layers on BAM surface: about 3, 5 and 10 atomic layers corresponding to the reaction time 1 min, 3 min and 5 min respectively. We will denominate the three different samples as C3-BAM, C5-BAM and C10-BAM in the remainder of this paper. The distances between every two layers are approximately 0.34 nm on average. Compared with the layer distance of graphite, the value here matches well with that of traditional graphite. Therefore, the coated layers on BAM particle may be similar to multilayer graphene.[18]

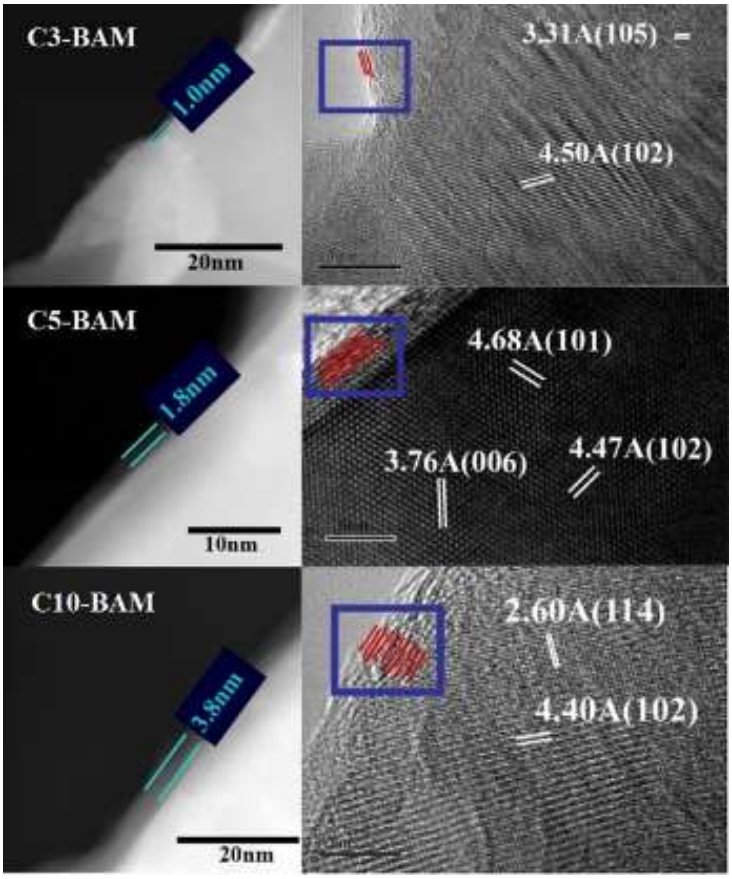

Figure 2. DF-STEM and HRTEM images of carbon-coated BAM.

The EDS results of C3-BAM, C5-BAM and C10-BAM samples are provided in Figure S1. They show that the products are all composed of C, Ba, Al, Mg, Eu, O. With the increase of the reaction time, higher carbon amount is observed. This conclusion agrees well with the above DF-STEM and HRTEM results.

Encapsulating a particle will prevent direct contact with the environment. Theoretically, the coating of BAM phosphor particles will absorb excitation radiation as well as emitted radiation. Hence, the emission intensities of most phosphor particles will decrease after covering their surface with a coating layer.[15, 19] The effect of carbon coating on the incident light can be preliminarily evaluated by the refractive index. Starting from the general equation, the refractive index *n* can be expressed as follows: [20]

$$\frac{4\pi k}{\lambda} = -\frac{1}{nd}\left[\frac{I}{I_0}\frac{1}{(1-R)}\right]$$

Where *k*, λ, *d* refer to the extinction coefficient, wavelength and thickness; *I*, I_0 and *R* are the transmitted light intensity, incident light intensity and the fraction of reflected light respectively. Therefore, it is difficult to determine the refractive index of multilayer graphene at a special wavelength band and so far this value is still under debate.[20-24] Here, the refractive index of carbon (2.0) is chosen to assess the total reflectivity change before and after carbon coating because the refractive index of carbon is almost located in the range $2 \sim 3$.[21] According to the further calculation with the refractive index (n) of air (1.0), C (2.0), and BAM phosphor (1.7), the reflectivity between air and the BAM phosphor is about 0.067, whereas the total reflectivity of carbon coated BAM (0.147) calculated from the air and C (0.111), and C and BAM phosphor (0.036), which means that the reflectivity of the carbon-coated BAM phosphor becomes greater and should have a negative influence on the incident light. The effect of carbon coating on the absorption of phosphors is evaluated experimentally by the reflection spectra, as shown in Figure 3. Absorption bands occur at 270, 310, and 390

nm respectively, which originate from Eu^{2+} $4f^7$ to $4f^65d^1$ electron transitions. It is found that an obvious decrease in absorption of C5-BAM does not happen, which disagrees with the analysis based on calculated reflectivity. This is probably due to the removal of surface defects by carbon coating on BAM, which will be discussed later. According to the Lambert–Beer law:

$$I = I_0 e^{-kd}$$

where I, I_0, k and d are the transmitted light intensity, incident light intensity, absorption coefficient and intermedium thickness respectively. Therefore, with further increase of the carbon layers to 10, the reflectivity of C10-BAM phosphor becomes much smaller over the whole visible spectral range, due to the considerable absorption by the residual carbon.

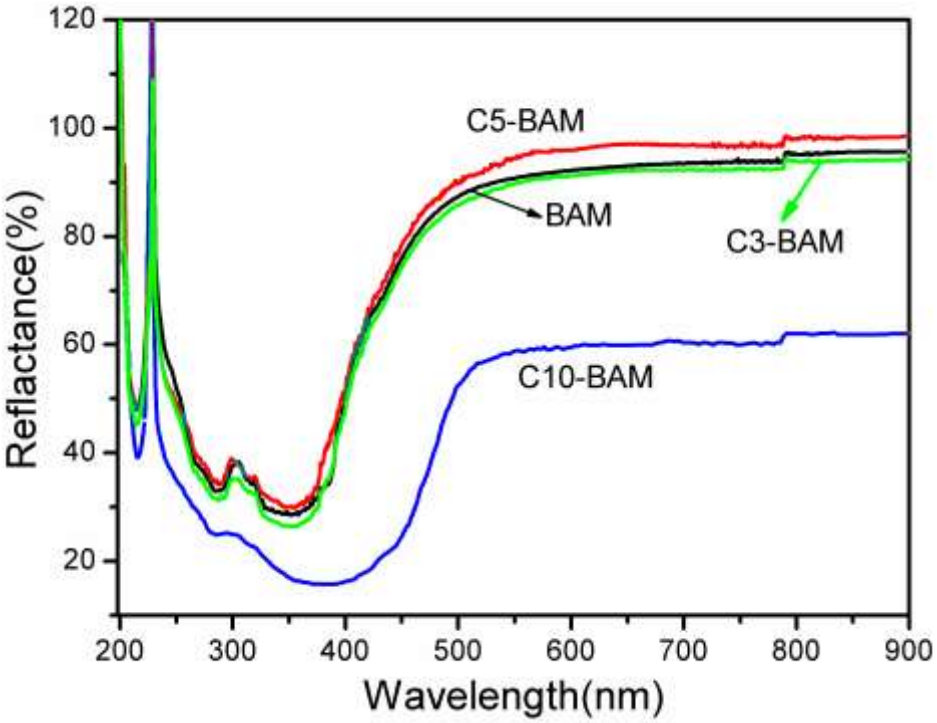

Figure 3. Reflection spectra of carbon coated and uncoated BAM, a small step in reflection curves at 800 nm is due to the switch of light source.

Figure 4 shows the excitation and emission spectra of C3-BAM, C5-BAM, C10-BAM and uncoated BAM phosphors for comparison. All emission spectra consist of a wide band with the peak at about 458 nm due to the transition from the $4f^65d^1$ excited state to the $4f^7$

ground state of Eu^{2+}, indicating that the local coordination of activator ions on the Ba^{2+} sites in BAM host is unchanged after coating. In addition, the blue emission intensity of C3-BAM and C5-BAM surpasses that of the uncoated BAM by 20% and 25%, respectively, while the intensity of C10-BAM is significantly lower than that of the uncoated. To eliminate the effect of heat-treatment on the emission intensity between BAM and carbon coated BAM, BAM is heat-treated under the same conditions without C_2H_2 reaction gas. It is found that the emission intensity is almost equal to original BAM (3% intensity discrimination), indicating this intensity change can indeed be ascribed to carbon coating instead of heat-treatment. The phenomenon reflects that the intensity of the carbon coated BAM can be increased by accurate controlling the coating layer. Combined with the result of reflectance spectra with almost the same intensity between C3-BAM, C5-BAM and uncoated BAM, it seems that the luminescence is more efficient in C3-BAM and C5-BAM than in uncoated BAM. The quantum efficiency (QE) of BAM and carbon-coated BAM is determined under 330 nm excitation, as shown in Table 1. Taking C5-BAM as an example, the internal and external QE of C5-BAM reaches 94.8% and 76.2% at room temperature respectively, which is higher than 91.1% and 65.4% of BAM.

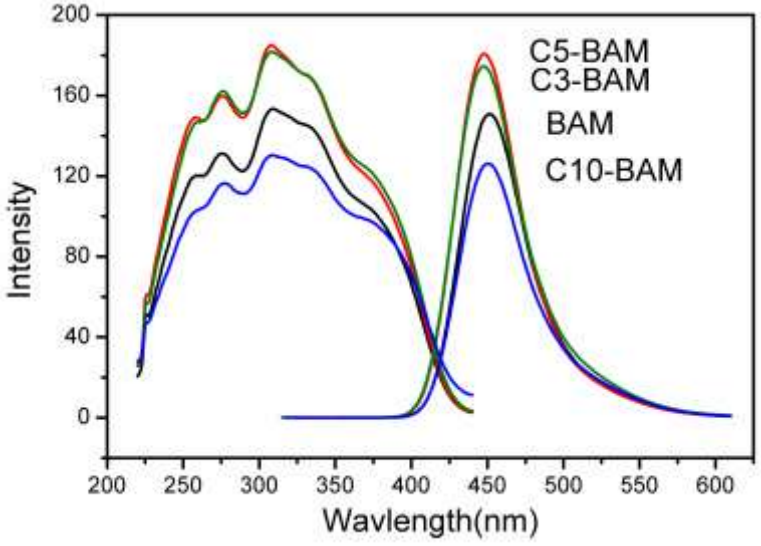

Figure 4. Excitation and emission spectra of carbon coated BAM and uncoated BAM phosphors. The excitation and monitoring wavelengths are 310 and 458 nm respectively.

Table 1. Emission intensity degradation and quantum efficiency of BAM phosphors with different carbon layers after heat-treatment at 600 °C for 0-2 h in air. η_i, η_o (0 h) represents the internal quantum efficiency (η_i) and external quantum efficiency (η_o) of samples without heat-treatment under 330 nm excitation. η_i, η_o (2 h) represents the internal quantum efficiency (η_i) and external quantum efficiency (η_o) of samples with heat-treatment at 600 °C for 2 h in air under 330 nm excitation.

Sample	0h	0.5h	1h	2h	η_i, η_o (0h)	η_i, η_o (2h)
BAM	0	7.2%	13.8%	20.4%	91.1%, 65.4%	73.4%, 51.7%
C3-BAM	0	1.0%	2.1%	4.3%	93.1%, 73.3%	85.8%, 68.4%
C5-BAM	0	2.5%	4.6%	5.2%	94.8%, 76.2%	86.2%, 68.3%
C10-BAM	0	0.8%	1.6%	1.3%	79.6%, 49.6%	78.0%, 49.3%

As mentioned earlier, the as-prepared layers may be made up of a carbon compound similar to graphene. It is well known that single layer graphene has a high light transmittance up to 97.7% for ultraviolet-visible light.[25-26] In other words, light transmittance will decrease by 2.3% with increase of every layer of grapheme. Hence, it will not have much influence on the absorption of the phosphor if the layer is limited to small thickness, i.e. 1-5 layers. Consequently the carbon coating will not show significant influence on the emission spectrum of BAM. Nevertheless, light transmittance may largely decrease by more than 20% when the number of layers reaches 10, which will evidently reduce the light reaching the BAM particle. It is why weaker luminescence intensity and lower quantum efficiency is exhibited for C10-BAM. It also explains that the difference in color of the carbon-coated BAM phosphors with different coating layers. C3-BAM and C5-BAM still remain white, whereas C10-BAM turns grey.

Phosphor powders typically have more defects near the surface, which work as a

luminescence quencher decreasing the luminescence efficiency of the phosphor. The SEM images in Figure S2 show that rough surface of uncoated BAM becomes smoother and clearer as the number of carbon layers increases. Furthermore, it is clearly seen that carbon particles exist on the surface of BAM, as shown in the high-magnification SEM image of C10-BAM. The enhancement of emission intensity under the same excitation conditions observed in the carbon-coated BAM may be ascribed to higher luminescence efficiency due to lower amounts of defects at the surface of the coated BAM phosphors than of the uncoated BAM phosphors, leading to the decrease of non-radiative transitions.

Besides the direct SEM observations, the micro surface change after carbon coating can be better reflected by decay time. The fluorescence lifetime is determined by the transition probability, which can be expressed as:

$$P_{(tot)} = P_{(rad)} + P_{(non-rad)} + \cdots \quad (1)$$

The change of luminescence efficiency can be characterized by the decay time τ(tot), which is given as:[27]

$$\tau_{(tot)}^{-1} = \tau_{(rad)}^{-1} + \tau_{(non-rad)}^{-1} \quad (2)$$

Here $\tau_{(rad)}$ and $\tau_{(non\text{-}rad)}$ is the radiative and non-radiative decay time, while $\tau_{(non\text{-}rad)}$ can be written as:

$$\tau_{(non-rad)}^{-1} = \tau_{(non-rad,bulk)}^{-1} + \tau_{(non-rad,surface)}^{-1} \quad (3)$$

where $\tau_{(non\text{-}rad,bulk)}$ and $\tau_{(non\text{-}rad,surface)}$ represent the non-radiative decay time via the bulk defect states and the surface states, respectively. It is expected that $\tau_{(rad)}^{-1}$ and $\tau_{(non\text{-}rad,bulk})^{-1}$ are hardly changed in the process of carbon coating because the coating temperature (600 °C) is much lower than the synthesis temperature of BAM (1500 °C). By the coating, large numbers of unpaired dangling bonds and defects on the surface of the BAM particles are removed. $\tau_{(non\text{-}rad,surface)}^{-1}$ will decrease once upon the surface defects are prohibited or passivated by carbon coating. Thus, the decrease of $\tau_{(non\text{-}rad,surface)}^{-1}$ results in a longer $\tau_{(tot)}$. This is indeed observed in the decay curve of Figure 5, showing that the decay time is lengthened to a minor

extent for carbon coated BAM (～1450 ns) as compared to uncoated BAM (1270 ns). From the above analysis, it can be concluded that the enhancement of luminescence efficiency originates from the reduction of the surface defects by carbon coating. Another interesting point is that the decay time of carbon coated BAM shows an increasing trend when increasing the number of the coated carbon layers (C3 < C5 < C10) by changing the deposition condition, although this change is very minor. For the reaction temperature of 600 °C, BAM surface is not fully covered by single carbon layers and there are possibly some cracks within the layers. Therefore, more carbon layers on BAM particles lead to a higher probability of full coverage on BAM surface and remove more surface defects, which lengthen the decay time.

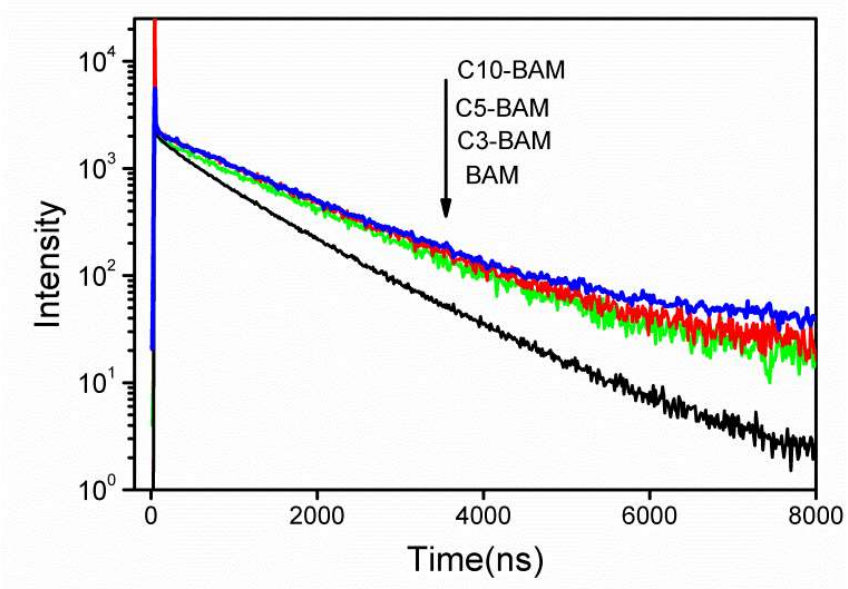

Figure 5. Decay curves of the emission wavelength at 458 nm in carbon-coated and uncoated BAM phosphors under 330 nm excitation.

BAM, one of the famous plasma display phosphors, will experience several heat treatments and undergo serious oxidation of Eu^{2+} during the PDP manufacturing process at the working temperature up to 500°C–600°C in air. So it is necessary to evaluate the thermal degradation properties of the samples heat-treated at 600 ^{o}C in air. Figure 6 shows the luminescence degradation of uncoated BAM, C3-BAM, C5-BAM and C10-BAM phosphors after heat treatment at 600 °C for 2 h in air. Figure 6(a) only shows the results of C5-BAM and pure

BAM as a comparison, and all the details are shown in Figure S3. Except for C10-BAM, other three kinds of BAM phosphors show the similar behavior – a decrease in luminescence intensity after the heat treatment as expected. The decrease of the intensity after high-temperature treatment can be linked to the decrease in the Eu^{2+} ion concentration which the formation of Eu^{3+} will act as killer center for Eu^{2+} luminescence and to the local structure change surrounding the Eu^{2+} ions. As BAM has a layered structure in which Eu^{2+} ions are sandwiched in between the spinel blocks, Eu^{2+} ions are thus easily attacked by oxygen. The oxidation mechanism during baking in air takes place in three sequential steps: 1) the adsorption of O_2 at the phosphor surface followed by incorporation of an oxygen atom into an oxygen vacancy, 2) the diffusion of Eu^{2+} ions along the conduction layer, and 3) the electron transfer from a Eu^{2+} ion to an oxygen atom incorporated in the oxygen vacancy when the two species are close to each other. As a result, part of the Eu^{2+} ions are oxidized to Eu^{3+} ions and the O atom will be reduced to O^{2-} ion. From our results it is evident that the thermal degradation is effectively suppressed by coating carbon on the BAM phosphor particles. Figure 6(b) exhibits the comprehensive effect of different carbon layers on thermal degradation of BAM phosphors. After heat treatment at 600 °C for 2 h in air, original BAM phosphor shows a 20% decrease in luminescence intensity; whereas C3-BAM only shows a 4.6% decrease, and C5-BAM only decreases 6.3%. Besides, an interesting phenomenon is that the intensity of C10-BAM after heat treatment for 2 h in air maintains consistent and even increases a little. The internal and external QE of C5-BAM only decreases by 9.1% and 10.3% after heat treatment, which is smaller than 19.4% and 20.9% of BAM. To make it clearer, the details are given in Table 1. From the results above, it is evident that the oxidation resistance of carbon coated BAM is much higher than that of uncoated BAM.

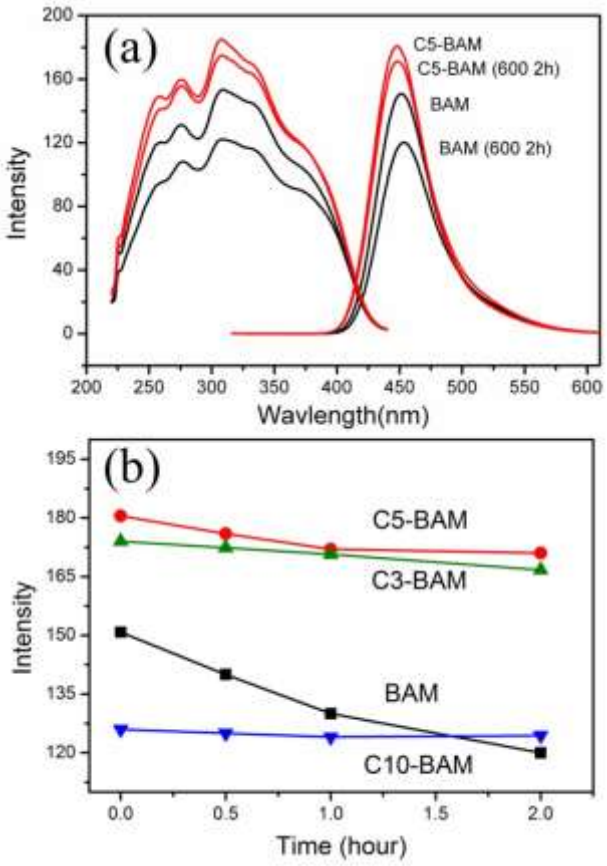

Figure 6. (a) Excitation and emission spectra of carbon-coated and uncoated BAM phosphors before and after heat treatment at 600 °C for 2 h in air. The excitation and monitoring wavelengths are 310 and 458 nm respectively. (b) The spectra of emission intensity after heat treatment at 600 °C for 0.5 – 2.0 h in air.

In order to find out what exactly happened to the carbon-coated BAM phosphor, we recorded HRTEM images for the annealed C5-BAM and C10-BAM in Figure 7. It can be visualized that the heat treatment does cause significant changes in the carbon layers. In Figure 7 (a), one can see that the carbon layers of the heat-treated C5-BAM become thinner. As observed in the amplified fine structure (indicated by rectangles), the carbon layers seem to disappear. The same is true for C10-BAM in Figure 7(b). Note that the carbon layers of the annealed C10-BAM become thinner and the surface is clearly non-uniform. In addition, the surface shows voids and pores formed by the escaping gases as observed in the amplified fine structure, which indicates the oxidation of carbon according to the reaction:

$$2C(s) + O_2(g) \rightarrow 2CO(g) \quad (4)$$

After thermal oxidation treatment, the carbon layers are still present on the BAM surface to play the role of preventing the entrance of oxygen to some extent.

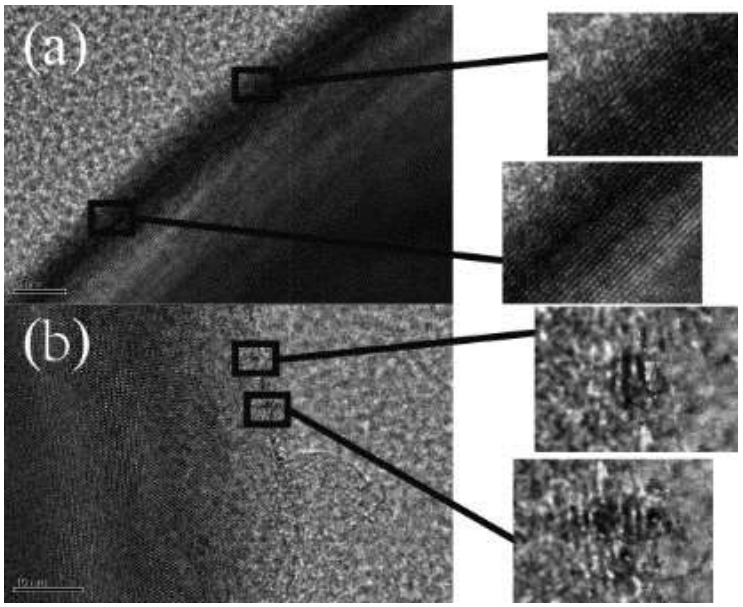

Figure 7. HRTEM images of (a) C5-BAM and (b) C10-BAM after heat treatment at 600 °C in air.

Figure 8 shows the direct evidence of the protection effect of carbon layers on Eu^{2+} valence as shown in Eu L_3-edge XANES spectra of BAM, C5-BAM and C10-BAM phosphors before and after heat treatment. Two peaks can be clearly seen at about 6977 and 6984 eV, which are due to the divalent and trivalent oxidation states of europium ions, respectively. All the non-heat-treated samples basically show the same characteristic that Eu^{2+} dominates. Eu^{2+} is oxidized into Eu^{3+} after 2 h heat treatment at 600 °C in air. However, the oxidation degrees differ from each other before and after carbon coating. More carbon layers around BAM phosphors result in the better thermal stability. The relative intensities of the peaks at 6977 and 6984 eV ascribed to Eu^{2+} and Eu^{3+} for the samples suggest that the oxidation degree of Eu^{2+} is greatly released by the help of carbon coating on BAM particles in the thermal treatment process.

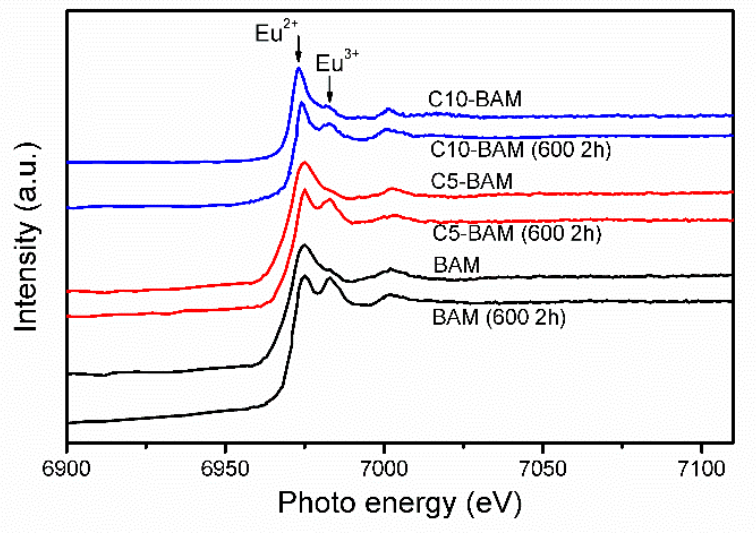

Figure 8. Eu L3-edge XANES spectra of BAM, C5-BAM and C10-BAM phosphors before and after heat treatment at 600 °C in air for 2 hours.

As discussed above, thermal degradation is caused by the oxidation of phosphors, which is also taking place for $Sr_2Si_5N_8$: Eu^{2+} and $SrSi_2O_2N_2$: Eu^{2+} phosphors.[28-29] In order to minimize the thermal degradation, it is of great importance to protect phosphors from oxidation; this can be done by surface coatings. The thermal degradation mechanism is schematically illustrated in Figure 9. Thus, the better thermal oxidation resistance of carbon-coated BAM may be attributed to the following reason: the surface coating prevents oxygen from entering the BAM particles. That is to say, in the first step of the degradation mechanism, the oxygen molecule (O_2) is not able to be adsorbed on the phosphor surface and subsequently be incorporated in the oxygen vacancy. Without the incorporated oxygen atom, the diffusion of Eu^{2+} ions along the conduction layer will not happen. Under this condition, oxygen from the air will have few chances to oxidize Eu^{2+} to Eu^{3+}. This explains the low degree of Eu^{2+} oxidation and the high thermal oxidation stability of carbon-coated BAM.

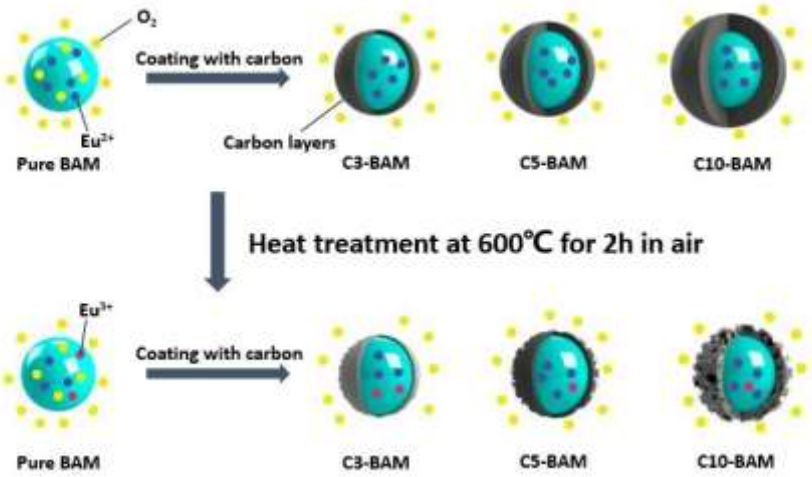

Figure 9. A schematic picture showing the protection mechanism of carbon coated BAM against thermal degradation in air.

CONCLUSION

Carbon coated BAM phosphor powders have been successfully prepared by a simple CVD method using C_2H_2 as a carbon source. EDS-mapping and TEM results show that a homogeneous carbon layer is successfully coated on the surface of BAM particles. The coating thickness can be tuned by setting the reaction time. The coated BAM phosphor exhibits higher emission intensity than that of the uncoated BAM phosphor due to a higher luminescence efficiency as a consequence of the removal of defects on the surface of BAM particles. Besides, this approach offers a low-cost method to get a more stable BAM, which can also be applied to the improvement of thermal degradation of other commercial phosphors.

ASSOCIATED CONTENT

Supporting Information

This information is available free of charge via the Internet at http://pubs.acs.org.

AUTHOR INFORMATION

Corresponding Author

*E-mail: ylj@mail.ustc.edu.cn, +31 653464032 (Liangjun Yin); jianxian@uestc.edu.cn, +86 13648079577 (Xian Jian).

Author Contributions

The manuscript was written through contributions of all authors. All authors have given approval to the final version of the manuscript. Liangjun Yin and Juntao Dong contributed equally to this paper.

Notes

The authors declare no competing financial interest.

ACKNOWLEDGMENT

This research was supported by the National Natural Science Foundation of China (Grant No. 51302029, 51402040) and the project-sponsored by OATF of UESTC and CSC. The authors thank Shanghai Synchrotron Radiation Facility for providing the XANES measurements. The authors thank Dr. Yongfu Liu for supporting QE measurements from Ningbo Institute of Materials Technology and Engineering (NIMTE).

REFERENCES

(1) Zhang, S.; Kono, T.; Ito, A.; Yasaka, T.; Uchiike, H. Degradation Mechanisms of the Blue-Emitting Phosphor $BaMgAl_{10}O_{17}:Eu^{2+}$ under Baking and Vuv-Irradiating Treatments. *J. Lumin.* **2004**, *106*, 39-46.

(2) Moine, B.; Bizarri, G. Why the Quest of New Rare Earth Doped Phosphors Deserves to Go On. *Opt. Mater.* **2006**, *28*, 58-63.

(3) Justel, T.; Krupa, J. C.; Wiechert, D. U. Vuv Spectroscopy of Luminescent Materials for Plasma Display Panels and Xe Discharge Lamps. *J. Lumin.* **2001**, *93*, 179-189.

(4) Bizarri, G.; Moine, B. On $BaMgAl_{10}O_{17}:Eu^{2+}$ Phosphor Degradation Mechanism: Thermal Treatment Effects. *J. Lumin.* **2005**, *113*, 199-213.

(5) Wang, Y.; Xu, X.; Yin, L.; Hao, L. High Thermal Stability and Photoluminescence of Si-N-Codoped $BaMgAl_{10}O_{17}:Eu^{2+}$ Phosphors. *J. Am. Ceram. Soc.* **2010**, *93*, 1534-1536.

(6) Kim, K. B.; Koo, K. W.; Cho, T. Y.; Chun, H. G. Effect of Heat Treatment on Photoluminescence Behavior of $BaMgAl_{10}O_{17}:Eu^{2+}$ Phosphors. *Mater. Chem. Phys.* **2003**, *80*, 682-689.

(7) Howe, B.; Diaz, A. L. Characterization of Host-Lattice Emission and Energy Transfer in $BaMgAl_{10}O_{17} : Eu^{2+}$. *J. Lumin.* **2004**, *109*, 51-59.

(8) Wang, Y. f.; Wang, Y. f.; Gao, J. k.; Lee, M. H.; He, W.; Xu, X.; Hao, L. Y.; Chen, J. H. First-Principles Study on Enhanced Optical Stability of $BaMgAl_{10}O_{17}:Eu^{2+}$ Phosphor by Sin Doping. *Chin. J. Chem. Phys.* **2012**, *25*, 398-402.

(9) Liu, B.; Wang, Y.; Zhou, J.; Zhang, F.; Wang, Z. The Reduction of Eu^{3+} to Eu^{2+} in $BaMgAl_{10}O_{17}: Eu^{2+}$ and the Photoluminescence Properties of $BaMgAl_{10}O_{17}: Eu^{2+}$ Phosphor. *J. Appl. Phys.* **2009**, *106*, 053102.

(10) Liu, B.; Wang, Y.; Zhang, F.; Wen, Y.; Dong, Q.; Wang, Z. Thermal Stability and Photoluminescence of S-Doped $BaMgAl_{10}O_{17}$: Eu^{2+} Phosphors for Plasma Display Panels. *Opt. Lett.* **2010**, *35*, 3072-3074.

(11) Liang, C.; Zhang, C.; Dong, Y.; Cao, T.; Jiang, J.; He, J. Improving Thermal Stability of $BaMgAl_{10}O_{17}$: Eu^{2+} Phosphor. *J. Rare Earths* **2006**, *24*, 153-156.

(12) Jung, K. Y.; Lee, D. Y.; Kang, Y. C. Improved Thermal Resistance of Spherical $BaMgAl_{10}O_{17}$: Eu^{2+} Blue Phosphor Prepared by Spray Pyrolysis. *J. Lumin.* **2005**, *115*, 91-96.

(13) Ekambaram, S.; Patil, K. C. Synthesis and Properties of Eu^{2+} Activated Blue Phosphors. *J. Alloys Compd.* **1997**, *248*, 7-12.

(14) Chen, Z.; Yan, Y. W.; Liu, J. M.; Yin, Y.; Wen, H. M.; Liao, G. H.; Wu, C. L.; Zao, L. Q.; Liu, D. H.; Tian, H. M. et al. Microstructure and Luminescence of Surface-Coated Nano-$BaMgAl_{10}O_{17}$: Eu^{2+} Blue Phosphor. *J. Alloys Compd.* **2009**, *478*, 679-683.

(15) Zhu, H.; Yang, H.; Fu, W.; Zhu, P.; Li, M.; Li, Y.; Sui, Y.; Liu, S.; Zou, G. The Improvement of Thermal Stability of $BaMgAl_{10}O_{17}$: Eu^{2+} Coated with MgO. *Mater. Lett.* **2008**, *62*, 784-786.

(16) Teng, X. M.; Zhuang, W. D.; Huang, X. W.; Cui, X. H.; Zhang, S. S. Luminescent Properties of $BaMgAl_{10}O_{17}$: Eu^{2+} Phosphors Coated with Y_2SiO_5. *J. Rare Earths* **2006**, *24*, 143-145.

(17) Li, F.; Yang, Y.; Song, Y.; Wang, W.; Yang, W.; Yang, B. Photoluminescence Spectroscopic Study of $BaMgAl_{10}O_{17}$: Eu^{2+} Phosphor Coated with CaF_2 Via a Sol-Gel Process. *J. Spectrosc.* **2013,** *2013*, 312519.

(18) Xu, Y.; Bai, H.; Lu, G.; Li, C.; Shi, G. Flexible Graphene Films Via the Filtration of Water-Soluble Noncovalent Functionalized Graphene Sheets. *J. Am. Chem. Soc.* **2008**, *130*, 5856-5857.

(19) Kim, Y.; Kang, S. Multi-Functional Colored Coating of $BaMgAl_{10}O_{17}$: Eu^{2+} Phosphors with Cobalt-Doped Al_2O_3 Thin Films. *Appl. Phys. A-Mater. Sci. & Process.* **2010**, *98*, 245-248.

(20) Bruna, M.; Borini, S. Optical Constants of Graphene Layers in the Visible Range. *Appl. Phys. Lett.* **2009**, *94, 031901*.

(21) Wang, X.; Chen, Y. P.; Nolte, D. D. Strong Anomalous Optical Dispersion of Graphene: Complex Refractive Index Measured by Picometrology. *Opt. Express* **2008**, *16*, 22105-22112.

(22) Ni, Z. H.; Wang, H. M.; Kasim, J.; Fan, H. M.; Yu, T.; Wu, Y. H.; Feng, Y. P.; Shen, Z. X. Graphene Thickness Determination Using Reflection and Contrast Spectroscopy. *Nano Lett.* **2007**, *7*, 2758-2763.

(23) Gray, A.; Balooch, M.; Allegret, S.; De Gendt, S.; Wang, W. E. Optical Detection and Characterization of Graphene by Broadband Spectrophotornetry. *J. Appl. Phys.* **2008**, *104, 053109*.

(24) Blake, P.; Hill, E. W.; Castro Neto, A. H.; Novoselov, K. S.; Jiang, D.; Yang, R.; Booth, T. J.; Geim, A. K. Making Graphene Visible. *Appl. Phys. Lett.* **2007**, *91, 063124*.

(25) Nair, R. R.; Blake, P.; Grigorenko, A. N.; Novoselov, K. S.; Booth, T. J.; Stauber, T.; Peres, N. M. R.; Geim, A. K. Fine Structure Constant Defines Visual Transparency of Graphene. *Science* **2008**, *320*, 1308-1308.

(26) Kim, K. S.; Zhao, Y.; Jang, H.; Lee, S. Y.; Kim, J. M.; Kim, K. S.; Ahn, J. H.; Kim, P.; Choi, J. Y.; Hong, B. H. Large-Scale Pattern Growth of Graphene Films for Stretchable Transparent Electrodes. *Nature* **2009**, *457*, 706-710.

(27) Delsart, C.; Pelletier-Allard, N. Probabilities for Radiative and Nonradiative Decay of Pr^{3+} Ion in $LaAlO_3$. *J. Phys. C: Solid State Phys.* **1973**, *6*, 1277-1291.

(28) Yeh, C. W.; Chen, W. T.; Liu, R. S.; Hu, S. F.; Sheu, H. S.; Chen, J. M.; Hintzen, H. T. Origin of Thermal Degradation of $Sr_{(2-X)}Si_5N_8$:$Eu_{(X)}$ Phosphors in Air for Light-Emitting Diodes. *J. Am. Chem. Soc.* **2012**, *134*, 14108-14117.

(29) Wang, C. Y.; Xie, R. J.; Li, F.; Xu, X. Thermal Degradation of the Green-Emitting $SrSi_2O_2N_2:Eu^{2+}$ Phosphor for Solid State Lighting. *J. Mater. Chem. C* **2014**, *2*, 2735-2742.

TOC graphic

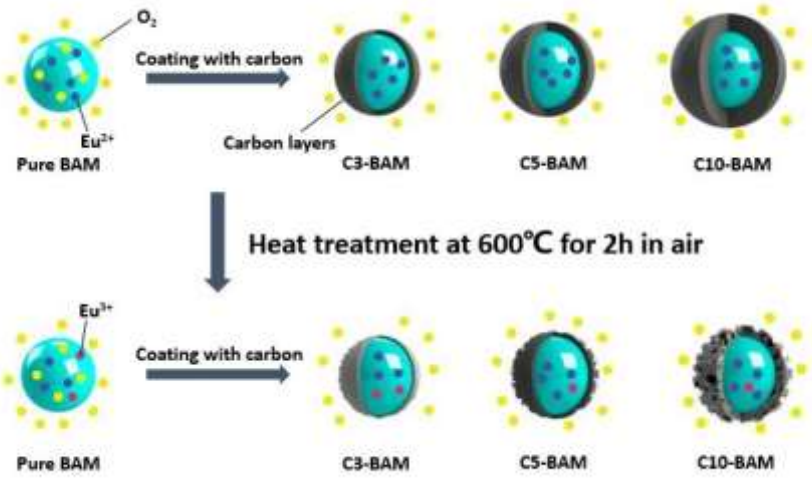
O2
Coating with carbon
Eu2+
Pure BAM
Carbon layers
C3-BAM
C5-BAM
C10-BAM
Heat treatment at 600℃ for 2h in air
Eu3+
Coating with carbon
Pure BAM
C3-BAM
C5-BAM
C10-BAM